

Review

# CBCT for Diagnostics, Treatment Planning and Monitoring of Sinus Floor Elevation Procedures

Nermin Morgan<sup>1,2,\*</sup>, Jan Meeus<sup>3</sup>, Sohaib Shujaat<sup>1,3,4</sup>, Simone Cortellini<sup>5,6</sup>, Michael M. Bornstein<sup>7</sup>  
and Reinhilde Jacobs<sup>1,3,8</sup>

- <sup>1</sup> OMFS IMPATH Research Group, Department of Imaging & Pathology, Faculty of Medicine, KU Leuven, 3000 Leuven, Belgium
  - <sup>2</sup> Department of Oral Medicine, Faculty of Dentistry, Mansoura University, Mansoura 35516, Egypt
  - <sup>3</sup> Department of Oral and Maxillofacial Surgery, University Hospitals Leuven, Campus Sint-Rafael, 3000 Leuven, Belgium
  - <sup>4</sup> King Abdullah International Medical Research Center, Department of Maxillofacial Surgery and Diagnostic Sciences, College of Dentistry, King Saud bin Abdulaziz University for Health Sciences, Ministry of National Guard Health Affairs, Riyadh 11426, Saudi Arabia
  - <sup>5</sup> Department of Oral Health Sciences, Section of Periodontology, KU Leuven, 3000 Leuven, Belgium
  - <sup>6</sup> Department of Dentistry, University Hospitals Leuven, KU Leuven, 3000 Leuven, Belgium
  - <sup>7</sup> Department of Oral Health & Medicine, University Center for Dental Medicine Basel UZB, University of Basel, 4058 Basel, Switzerland
  - <sup>8</sup> Department of Dental Medicine, Karolinska Institute, 141 04 Huddinge, Sweden
- \* Correspondence: nermin.morgan@student.kuleuven.be

**Abstract:** Sinus floor elevation (SFE) is a standard surgical technique used to compensate for alveolar bone resorption in the posterior maxilla. Such a surgical procedure requires radiographic imaging pre- and postoperatively for diagnosis, treatment planning, and outcome assessment. Cone beam computed tomography (CBCT) has become a well-established imaging modality in the dentomaxillofacial region. The following narrative review is aimed to provide clinicians with an overview of the role of three-dimensional (3D) CBCT imaging for diagnostics, treatment planning, and postoperative monitoring of SFE procedures. CBCT imaging prior to SFE provides surgeons with a more detailed view of the surgical site, allows for the detection of potential pathologies three-dimensionally, and helps to virtually plan the procedure more precisely while reducing patient morbidity. In addition, it serves as a useful follow-up tool for assessing sinus and bone graft changes. Meanwhile, using CBCT imaging has to be standardized and justified based on the recognized diagnostic imaging guidelines, taking into account both the technical and clinical considerations. Future studies are recommended to incorporate artificial intelligence-based solutions for automating and standardizing the diagnostic and decision-making process in the context of SFE procedures to further improve the standards of patient care.

**Keywords:** CBCT; three-dimensional imaging; maxillary sinus; sinus floor elevation; sinus floor augmentation



check for updates

**Citation:** Morgan, N.; Meeus, J.; Shujaat, S.; Cortellini, S.; Bornstein, M.M.; Jacobs, R. CBCT for Diagnostics, Treatment Planning and Monitoring of Sinus Floor Elevation Procedures. *Diagnostics* **2023**, *13*, 1684. <https://doi.org/10.3390/diagnostics13101684>

Academic Editor: Fabiano Bini

Received: 12 April 2023

Revised: 5 May 2023

Accepted: 6 May 2023

Published: 10 May 2023



**Copyright:** © 2023 by the authors. Licensee MDPI, Basel, Switzerland. This article is an open access article distributed under the terms and conditions of the Creative Commons Attribution (CC BY) license (<https://creativecommons.org/licenses/by/4.0/>).

## 1. Introduction

Alveolar bone atrophy in the maxillary posterior region is inevitable following tooth extraction, resulting in horizontal and vertical ridge resorption [1,2]. If a dental implant is inserted in bone having inadequate volume, there is a high risk of compromised implant stability and poor prognosis [3,4]. In order to compensate for reduced bone height and volume of the maxillary posterior region, sinus floor elevation (SFE) is performed for bone reconstruction. It involves lifting up of the Schneiderian membrane, which is usually followed by the placement of a bone graft [5–9].

The two main techniques for SFE are either a direct approach using a lateral window or indirect with the transalveolar technique. In the lateral window approach, an osteotomy

is performed in the buccal wall of the maxilla, creating access through the lateral bone wall of the sinus cavity [10–12]. The transalveolar technique is a less invasive technique that was modified by Summers [13], where a transcresal osteotome is applied to elevate the sinus floor, pushing bone substitutes beyond the level of the original sinus floor [14]. This technique has been recommended in areas with sufficient alveolar crest width and where a residual vertical bone height of  $\geq 5$  mm is available [15]. In cases where the alveolar bone height is less than 5 mm, the lateral window approach is recommended [16].

To date, various graft materials have been successfully used for SFE solely or in combination with each other [17], such as autograft [18–21] (intraoral: chin, retromolar region, mandibular ramus, maxillary tuberosity [22,23]; extraoral: iliac crest, fibula, tibia [24–26]), allograft [27–29] (fresh, frozen, freeze-dried bone [30,31]), xenograft [32–36] (deproteinized bovine bone [37–39]), and phylogenetic material [39–41] (Gusuibu, coral-based bone substitutes, and marine algae).

Along with patient history and clinical examination, radiographic examination is an essential component of preliminary diagnostics, treatment planning, and outcome assessment in patients requiring SFE. Previously, two-dimensional (2D) panoramic radiography acted as a clinical standard. However, it suffers from certain inherent limitations, which can negatively impact the task at hand, such as magnification, distortion, and superimposition [16,42].

Three-dimensional (3D) preoperative imaging of the specific site of augmentation becomes a prerequisite in order to provide needed information about the morphologic characteristics and/or pathological conditions of the sinus and residual ridge [43–45]. Some studies have used computed tomography (CT) for the planning of sinus grafting [46] and precalculated the augmented bone volume needed [47–50]. However, the use of CT imaging is limited for most dental practitioners due to the high costs, large size of the device, and high radiation dose. To overcome these general limitations, 3D imaging in the form of cone beam CT (CBCT) has become a standard [43,44] for patients requiring maxillary sinus procedures. Recently, various CBCT imaging systems with low-dose protocols have also been made commercially available, which are not only affordable and compact to be used in a private dental practice but also provide 3D imaging with a lower radiation dose exposure to the patient [51,52].

The aim of the present review was to discuss the role of CBCT imaging for diagnostics, treatment planning, and postoperative monitoring of SFE as well as recommend future research directions, which could be useful for improving the current standard of patient care.

## 2. Use of CBCT for Diagnostics and Treatment Planning Prior to SFE

CBCT has been widely employed for diagnosis and preoperative treatment planning in all fields of dentistry [53], allowing for 3D visualization of dental structures and multiplanar reconstruction. It can provide cross-sectional images of the alveolar bone with the ability to accurately measure its height, width, and depict surrounding vital structures, such as the maxillary sinus. It allows for thorough assessment of the bone quality (density) and quantity (thickness) as well as the detection of bony changes, such as fractures or malformations. Furthermore, CBCT can be used for volume quantification that could help monitor bone remodeling and sinus disease [45,53,54].

Based on the recommendations of the American Academy of Oral and Maxillofacial Radiology (AAOMR) [55], CBCT imaging prior to SFE provides surgeons with a more detailed view of the surgical site. This helps to plan the surgical intervention more precisely while reducing patient morbidity. Additionally, it can be used to detect any potential problems and/or present pathology in advance, allowing for a safer and more successful bone grafting procedure. This also comes in accordance with the consideration of sinus augmentation mentioned in the updated guidelines for the use of diagnostic imaging in implant dentistry published by the European Association for Osseointegration (E.A.O.) [56].

From a technical point of view, in patients requiring CBCT acquisition for diagnostics, the “as low as reasonably achievable” (ALARA) principle has gone through a long

history of evolution. Recently, some expert opinions advocated to rename it to “as low as diagnostically acceptable” (ALADA) [57] and, more recently, “as low as diagnostically acceptable being indication-oriented and patient-specific” (ALADAIP) [58]. These up to date principles highlight the need for actually optimizing rather than simply minimizing doses, taking into account not only the diagnosis but also treatment planning such as preoperative sinus grafting. For instance, when there is evidence of sinus pathology or sinus drainage is expected to be impaired, which might jeopardize the SFE outcomes, it is justifiable to extend the field of view (FOV) to include the whole of the maxillary sinus, including the ostio-meatal complex [59–62].

Furthermore, a multitude of CBCT devices exist in the market with variable scanning parameters, which include slice thickness, FOV, mAs, kVp, and scan time [63]. All these factors influence the image quality and amount of administered radiation dose. Generally, the effective radiation doses of CBCT devices for maxillofacial applications should preferably be 20 to 100  $\mu\text{Sv}$ ; however, the doses of commercially available devices range from 10 to 1000  $\mu\text{Sv}$  depending on the parameter’s settings. Nevertheless, it is still lower than that of CT devices, which might vary between 474 and 1160  $\mu\text{Sv}$  [45,64]. Saying that, it is recommended to justify and optimize CBCT acquisition parameters for diagnostic tasks in an attempt to decrease the risk of high radiation dose exposure to the patient.

From a clinical point of view, CBCT enhances the diagnostic evaluation relative to 2D imaging by providing additional information related to the maxillary sinuses and surrounding structures. This diagnostic information could be a useful adjunct for SFE planning, as a thorough radiological assessment is not only important for the sinus surgery but also for implant placement. The diagnostic features extracted from CBCT images that could be clinically relevant for performing a successful SFE procedure, which could very well remain undetected with 2D imaging, are as follows:

- *Anatomy of maxillary sinus and alveolar ridge*

CBCT imaging provides detailed anatomical information related to sinus anatomy. These findings allow the surgeon to assess the sinus morphology, density, and volume of the residual alveolar ridge, which might in turn help to determine the best approach for accessing the sinus and to evaluate the suitability of the patient’s bone for grafting [55,65].

- *Relation of maxillary sinus to the roots of adjacent teeth*

If there is an intimate contact between the root(s) of the teeth and the Schneiderian membrane, the risk of membrane perforation during the sinus lift procedure is increased. Hence, it is important to evaluate the root proximity to the sinus during the diagnostic phase through CBCT imaging for decreasing the risk of perforation [66,67]. Additionally, the health state of adjacent teeth should be examined for the presence of pre-existing apical pathology that could result in sinus graft infection [68].

- *Thickness of the Schneiderian membrane*

CBCT has been reported to be a useful tool for assessing the thickness of the Schneiderian membrane [60,69], which has also been reported to be associated with the occurrence of membrane perforation [70]. Healthy sinus mucosa has a mean thickness of 1 mm, although there is a wide range of variability among individuals [71]. Meanwhile, it should be noted that the risk of sinusitis following SFE increases when the membrane thickness is over 2 mm [72], and a higher risk of ostium obstruction exists if the membrane thickness is over 5 mm [73].

- *Maxillary sinus septum [74,75]*

Prior evidence suggests that at least one-third of patients have sinus septa, which are visualized ideally through 3D imaging [76]. The knowledge about septa location and morphology is a key factor in planning SFE, as it is associated with an increased risk of sinus membrane perforation during the procedure. Furthermore, if present, the osteotomy design might also require an alteration from a single window technique to two smaller windows on either side of the maxillary sinus floor septum or the use of a W-shaped

trapdoor technique. Hence, CBCT imaging is the key to success in devising a proper treatment plan [77].

- *Maxillary sinus ostium*

Sinus healing following SFE is largely dependent on sufficient drainage of the nasal cavity. If the ostium is not patent, the drainage would be impaired, which could cause sinusitis or surgical failure [72]. For guaranteeing appropriate mucociliary drainage and clearance, the ostium patency must be evaluated prior to surgery. In addition, the sinus should be assessed for the presence of accessory ostia, which can interfere with sinus ventilation and drainage [78].

- *Maxillary sinus floor width*

The distance and angulation between the lateral and medial maxillary sinus walls are also important anatomical features to be evaluated with CBCT imaging. It allows determining the difficulty level of performing SFE, as too narrow or too large sinuses with sharp angulations are considered complex cases. Moreover, accurate measurement of the sinus width based on CBCT imaging is also crucial for deciding the surgical approach; for example, a trapdoor SFE technique is contraindicated in patients having narrow sinuses [79].

- *Thickness of the lateral maxillary sinus wall*

Maxillary sinus lateral wall thickness is an important parameter to be assessed using CBCT imaging at the diagnostic stage because SFE through a thick wall is difficult to perform, takes longer time and is more prone to perforation. Hence, CBCT imaging is suggested to help with the decision-making process, as it allows the surgeon to 3D evaluate the sinus wall and select the region with the least thickness to avoid complications [80].

- *Alveolar antral artery*

CBCT imaging allows a clear depiction of the antral artery, allowing for an optimal planning of the surgical access to the sinus. Alveolar antral arteries with a diameter more than 0.5 mm can be observed on CBCT, and profuse bleeding should be expected if the artery has a diameter more than 3 mm [81]. If present at the osteotomy site, the use of a piezosurgery device is preferred. Moreover, changing the osteotomy window design from an oval to a round shape through either above or below this artery could avoid injury [82].

- *Estimation of graft volume*

Using the combination of CBCT images along with the various planning software systems available allows for measuring and extracting the sinus volume necessary to be grafted [83]. Adequate preoperative planning of the graft volume may help to avoid sinus over-filling and potentially occluding the ostium, decide on the ratio of bone and bone substitutes to be mixed, and estimate the cost of xenografts prior to the actual operation [47,48]. It is worth noting that in cases where an autogenous graft will be harvested, preoperative knowledge of the amount of graft required is useful in selecting the optimal donor region, reducing the time and complexity of the surgical procedures, as well as minimizing potential postoperative complications [84].

- *Incidental findings*

The role of CBCT in revealing incidental findings (IFs) which are not related to the primary scan indication also cannot be ignored. Several studies have reported a high prevalence of IFs in the maxillary sinus region on CBCT images when acquiring the scan for the purpose of implant/surgical planning [85,86]. The most common IFs encompass concha bullosa, mucosal thickening, polyps, altered sinus dimensions, and sinus opacification. Some IFs may also be suggestive of benign or malignant neoplastic processes. Hence, it is important for the dental practitioner to be aware of these findings on CBCT images, which might allow a more appropriate selection of a treatment plan as patients with IFs might be predisposed to a higher risk of postoperative complications from SFE and implant

placement. Although a smaller FOV CBCT scan results in less radiation, the risk of missing IFs still exists. Hence, it is recommended to acquire a scan with an optimal FOV depending on the clinical indications and risk–benefit analysis. To reach a more definitive conclusion, more research is also needed to examine how different FOVs affect the incidence of IFs.

### 3. Digital Workflow for SFE Procedures

In recent years, digital technologies and workflows have been introduced in the majority of dental medicine fields, including restorative dentistry, orthodontics, dental implantology, and maxillofacial reconstructive surgery [87]. Digital treatment planning workflow refers to the incorporation of computer-controlled components and dental technologies for assisting a clinician with the planning process. This digitization of workflows in clinical dentistry has overcome the limitations associated with traditional methods by offering improved precision of dental procedures, time-efficiency, and a higher standard of patient care [88–90].

#### 3.1. Virtual Modelling

Generally, CBCT images are saved in a Digital Imaging and Communications in Medicine (DICOM) format, which is then transferred to 3D software programs for further processing to plan the procedure. The most essential step in SFE planning workflows is segmentation, a process by which the region of interest is extracted from 3D images for generating 3D virtual models. These models are then used for fabricating guides or pre-surgically assessing the amount of required (bone) graft (Figure 1).

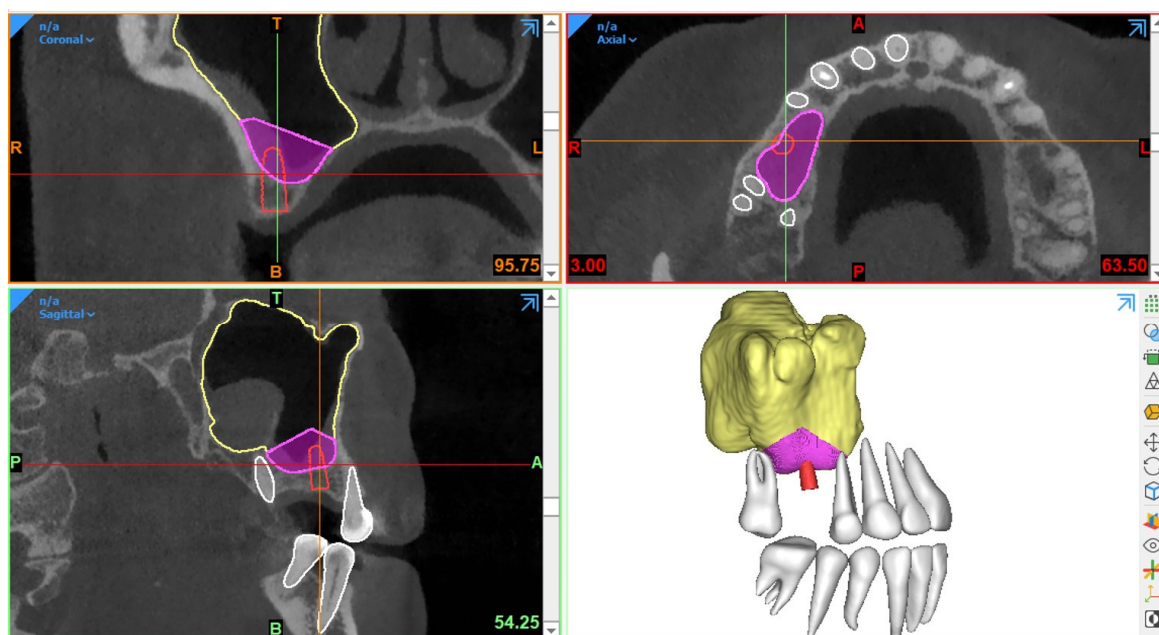


**Figure 1.** Example of graft volume estimation in Mimics (version 23.0, Materialise N.V., Leuven, Belgium) following automated sinus and teeth segmentation ([creator.relu.eu](https://creator.relu.eu), Relu, BV, Version March 2023).

Traditionally, manual sinus segmentation, referred to as slice-by-slice delineation on 2D CBCT planes, performed by an expert is considered the gold standard. However, it is prone to certain limitations, such as labor-intensiveness, increased time consumption, and observer variability [91,92]. Based on the aforementioned limitations, semi-automated segmentation via thresholding-based approaches has been widely adopted for the segmentation of CBCT images to improve the efficiency of planning workflows [93,94]. Nevertheless, the final segmentation lacks optimal delineation due to the presence of different structural densities, and manual post-processing is often required. Recently, artificial intelligence (AI) in the form of deep learning has been employed for automated segmentation to overcome

the limitations associated with both manual and semi-automated segmentation approaches. In deep learning, convolutional neural networks (CNNs) have demonstrated excellent performance with the employment of multi-layer neural computational connections for sinus segmentation on CBCT images [95–97]. The application of such deep learning-based approaches might enhance the quality and predictability of presurgical graft planning, enable a more precise treatment planning process and volumetric quantification of sinus/graft changes, and may further improve the standard of care. Yet, a lack of evidence exists related to the application of AI in the SFE treatment planning workflows.

### 3.2. Surgical Guidance

In SFE procedures, CBCT-based guidance has played a vital role in improving the precision of the surgical procedure with a reduction in complications. The guidance can be static or dynamic in nature. The procedures performed via these guides are referred to as “guided sinus lift [98]” or “guided bone grafting [99]”.

#### 3.2.1. Static Surgical Guides

Static guides are designed via 3D planning software programs following the integration of intraoral scanned images with CBCT datasets and later fabricated using 3D printers. Such surgical templates act as a support aid and offer the advantages of time-efficiency, better working ergonomics, less operator stress, and greater predictability of the procedure [98,100,101]. Moreover, this procedure can also be combined with concurrent implant placement planning.

In 2008, Manderales and Rosenfeld [99] pioneered computer-guided SFE. They proposed using CAD/CAM surgical cutting guides for exact lateral wall outlining to considerably improve the quality and outcomes of the SFE procedure. Cecchetti et al. [98] have recently introduced virtual planning of surgical guides for lateral wall sinus elevation, concluding that the surgical template should be seen as a support aid to minimize risk and complications of the surgical procedures, especially in “difficult” cases.

Following the same concept, Osman et al. [102] and Strbac et al. [101] performed computer-guided SFE through a lateral window approach in addition to simultaneous implant placement. They found that applying static guides resulted in better and more consistent results. Similarly, Pistilli et al. [100] also concluded that such a digital approach is highly efficient in the mid-term (follow-up of 10 years) to implant rehabilitation of severely resorbed maxilla simultaneously with sinus lift.

Considering transrectal sinus augmentation, Pozzi et al. [103] and An et al. [104] combined static guide-based flapless maxillary crestal sinus augmentation with an immediate nonfunctional loading of dental implants, reporting a 98.53% and 100% survival rate at 3 years and 37 months, respectively.

Another type of surgical guidance is dynamic navigation, which is based on computer-guided surgery planning. Here, a physical surgical guide is unnecessary [105].

#### 3.2.2. Dynamic Surgical Guides

A dynamic navigation system combined with CBCT imaging has been proposed for improving the intraoperative precision of implant placement, where a static surgical guide is not required and the operator can place the implants with real-time navigation [106]. With regard to SFE, limited evidence exists related to the application of navigation-based approaches. Recently, dynamic navigation has been used for posterior maxilla implant surgery via transcresal SFE using piezoelectric devices [107]. The proposed technique offered high precision with excellent clinical outcome. However, it is recommended to perform further clinical studies to assess the effectiveness of dynamic navigation for performing SFE.

Considering the intraoperative use of CBCT imaging, Blake et al. [108] performed one case trial of using a C-arm-based CBCT scanner during sinus augmentation surgery under general anesthesia with iliac crest grafting. The images were taken prior to wound

closure to immediately verify the surgery result. However, there is no solid evidence regarding such procedures for surgeries performed under local anesthesia.

#### 4. Use of CBCT for Monitoring and Follow-Up after SFE

Post-surgical radiographic examination is vital [19,49,109–121] for the evaluation of bony integration of the inserted graft, follow-up of its long term stability, and also assessment of implant success and/or osteointegration after sinus lift procedures.

Ideally, imaging guidelines for the follow-up of sinus augmentation with or without immediate implant placement should follow the same regulations as those for post-surgical implant placement. Based on the AAOMR recommendations [55] and the guidelines for the use of diagnostic imaging in implant dentistry published by the E.A.O. [56], intraoral periapical radiography should be performed for the postoperative assessment of implants in the absence of clinical signs or symptoms. Panoramic radiographs may be indicated for more extensive implant therapy cases.

Meanwhile, CBCT [109,112,115] has become the standard imaging technique for 3D visualization and improved assessment prior to implant placement in the case of staged sinus augmentation. CBCT imaging can help to assess bone healing by visualizing how the material has integrated with the surrounding bone as well as if any signs of early resorption exist. It is beneficial in providing information about the volume, extent, and density of the augmented region [56] and can also be used to monitor any complications, which are not visible to the naked eye, such as mucosal changes, infection, and/or inflammation.

Furthermore, bone graft materials undergo remodeling over time at varying rates depending on the material used (resorbable versus non-resorbable) [122], and positive pressure formed inside the sinus during respiration also accelerates graft resorption [123]. Certainly, this remodeling could have a significant impact on the success of SFE outcome and the respective implant treatment. Thereby, CBCT can aid in the quantification of the resorption rate of different grafting materials [124–126] and also to monitor sinus changes at follow-up stages by comparing pre-surgical and/or post-surgical scans acquired at different time points. Usually, the Schneiderian membrane exhibits significant post-surgical edema, which increases the mucosal thickness visible. In addition, the edema might cause ostium obstruction with the possibility of impaired drainage capacity of sinus mucus. The reduction in the patency and obstruction of the ostium and infundibulum can lead to an inflammatory reaction and/or infectious processes of the sinus cavity, causing acute or chronic sinusitis [127]. Hence, CBCT imaging could act as a useful follow-up assessment tool to measure the thickness of the membrane and monitor mucosal changes in an attempt to avoid both early and delayed postoperative complications [128]. Additionally, following up the mucosal thickness changes could help to study the possible effects of different graft materials on sinus mucosa for research purposes [129].

It should be kept in mind that the use of CBCT should not be opted for regular follow-up assessment of normal SFE procedures without any evident or suspected complications to avoid exposure to unnecessary radiation doses. Postoperative CBCT could be indicated in cases with complications and contraindicated in patients where no direct benefit is to be expected. In instances of no clinical signs or symptoms of treatment failure or complications, periapical or panoramic images could be considered more than enough for postoperative follow-up. Moreover, CBCT imaging should also be justifiable for ethically approved clinical research projects, which might improve the standard of patient care. However, optimized strategies still need to be developed for SFE follow-up assessment, allowing good image quality and accurate 3D modeling with low-dose scanning protocols.

#### 5. Recommendations and Future Developments

Maxillary sinus floor elevation is nowadays considered a safe and effective surgical technique to allow prosthetic restoration supported by implants in the atrophic posterior region of the maxilla. CBCT imaging has significantly improved the accuracy and efficiency of performing SFE procedures. It has become an imaging modality of choice for diagnostics

due to its potential for detecting challenging anatomical and/or pathological entities, which would probably remain undetected with 2D imaging. However, one should consider that in a private practice, it is difficult and time consuming for a dentist to identify all CBCT-based diagnostic parameters, which might negatively impact the decision-making process. Hence, future studies should attempt to integrate artificial intelligence-based solutions using CBCT images for automating and standardizing the diagnostic and decision-making process for performing SFE procedure.

In relation to treatment planning, automated AI-based CBCT image segmentation has already been implemented for the production of virtual models of maxillary sinuses and jawbone. However, still no evidence exists related to the integration of AI networks in the digital treatment planning workflows of SFE. Hence, future studies should also focus on investigating the accuracy and efficiency of these networks and models in treatment planning workflows. Furthermore, they should also investigate the combination of quantitative extracted features following image segmentation with biological, clinical, and demographic patient characteristics, which is referred to as “radiomics” [130]. Such a combination could be a step forward toward personalized dental medicine, enabling the best possible treatment for each patient [131,132].

As for follow-up assessments, it is recommended to perform studies comparing the 3D resorption rate associated with different surgical techniques and grafting materials and also assess the morphological changes of the sinus. Even for the post-surgical assessment of the sinus and grafted region, the application of AI allowing automated virtual modeling could be beneficial in an attempt to further improve the surgical outcomes and better understand the associated complications. As for the justification of CBCT imaging, there is a need for future research to establish an optimized low-dose CBCT protocol for SFE diagnostics, 3D planning, and follow-up assessment, which does not impair the image quality depending on the task at hand.

**Funding:** This research received no external funding.

**Institutional Review Board Statement:** Not applicable.

**Informed Consent Statement:** Not applicable.

**Data Availability Statement:** Data sharing is not applicable to this article.

**Conflicts of Interest:** The authors declare no conflict of interest.

## References

1. Chen, S.T.; Darby, I. Alveolar ridge preservation and early implant placement at maxillary central incisor sites: A prospective case series study. *Clin. Oral Implant. Res.* **2020**, *31*, 803–813. [[CrossRef](#)] [[PubMed](#)]
2. Hansson, S.; Halldin, A. Alveolar ridge resorption after tooth extraction: A consequence of a fundamental principle of bone physiology. *J. Dent. Biomech.* **2012**, *3*, 1758736012456543. [[CrossRef](#)] [[PubMed](#)]
3. Farmer, M.; Darby, I. Ridge dimensional changes following single-tooth extraction in the aesthetic zone. *Clin. Oral Implant. Res.* **2014**, *25*, 272–277. [[CrossRef](#)] [[PubMed](#)]
4. Jemt, T.; Lekholm, U. Implant treatment in edentulous maxillae: A 5-year follow-up report on patients with different degrees of jaw resorption. *Int. J. Oral Maxillofac. Implant.* **1995**, *10*, 303–311.
5. Bathla, S.C.; Fry, R.R.; Majumdar, K. Maxillary sinus augmentation. *J. Indian Soc. Periodontol.* **2018**, *22*, 468–473. [[CrossRef](#)] [[PubMed](#)]
6. Bornstein, M.M.; Chappuis, V.; Von Arx, T.; Buser, D. Performance of dental implants after staged sinus floor elevation procedures: 5-year results of a prospective study in partially edentulous patients. *Clin. Oral Implant. Res.* **2008**, *19*, 1034–1043. [[CrossRef](#)]
7. Del Fabbro, M.; Wallace, S.S.; Testori, T. Long-term implant survival in the grafted maxillary sinus: A systematic review. *Int. J. Periodontics Restor. Dent.* **2013**, *33*, 773–783. [[CrossRef](#)]
8. Esposito, M.; Felice, P.; Worthington, H.V. Interventions for replacing missing teeth: Augmentation procedures of the maxillary sinus. *Cochrane Database Syst. Rev.* **2014**, Cd008397. [[CrossRef](#)]
9. Starch-Jensen, T.; Jensen, J.D. Maxillary Sinus Floor Augmentation: A Review of Selected Treatment Modalities. *J. Oral Maxillofac. Res.* **2017**, *8*, e3. [[CrossRef](#)]
10. Boyne, P.J.; James, R.A. Grafting of the maxillary sinus floor with autogenous marrow and bone. *J. Oral Surg.* **1980**, *38*, 613–616.
11. Caudry, S.; Landzberg, M. Lateral window sinus elevation technique: Managing challenges and complications. *J. Can. Dent. Assoc.* **2013**, *79*, d101. [[PubMed](#)]

12. Tatum, H., Jr. Maxillary and sinus implant reconstructions. *Dent. Clin. N. Am.* **1986**, *30*, 207–229. [[CrossRef](#)] [[PubMed](#)]
13. Summers, R.B. A new concept in maxillary implant surgery: The osteotome technique. *Compendium* **1994**, *15*, 152, 154–6, 158 passim; quiz 162.
14. Temmerman, A.; Van Dessel, J.; Cortellini, S.; Jacobs, R.; Teughels, W.; Quirynen, M. Volumetric changes of grafted volumes and the Schneiderian membrane after transcrestal and lateral sinus floor elevation procedures: A clinical, pilot study. *J. Clin. Periodontol.* **2017**, *44*, 660–671. [[CrossRef](#)]
15. Wang, H.L.; Katranji, A. ABC sinus augmentation classification. *Int. J. Periodontics Restor. Dent.* **2008**, *28*, 383–389.
16. Mohan, N.; Wolf, J.; Dym, H. Maxillary sinus augmentation. *Dent. Clin. N. Am.* **2015**, *59*, 375–388. [[CrossRef](#)]
17. Zhao, R.; Yang, R.; Cooper, P.R.; Khurshid, Z.; Shavandi, A.; Ratnayake, J. Bone Grafts and Substitutes in Dentistry: A Review of Current Trends and Developments. *Molecules* **2021**, *26*, 3007. [[CrossRef](#)]
18. Johansson, L.A.; Isaksson, S.; Lindh, C.; Becktor, J.P.; Sennerby, L. Maxillary sinus floor augmentation and simultaneous implant placement using locally harvested autogenous bone chips and bone debris: A prospective clinical study. *J. Oral Maxillofac. Surg.* **2010**, *68*, 837–844. [[CrossRef](#)]
19. Klijn, R.J.; Meijer, G.J.; Bronkhorst, E.M.; Jansen, J.A. A meta-analysis of histomorphometric results and graft healing time of various biomaterials compared to autologous bone used as sinus floor augmentation material in humans. *Tissue Eng. Part B Rev.* **2010**, *16*, 493–507. [[CrossRef](#)] [[PubMed](#)]
20. Nkenke, E.; Stelzle, F. Clinical outcomes of sinus floor augmentation for implant placement using autogenous bone or bone substitutes: A systematic review. *Clin. Oral Implant. Res.* **2009**, *20* (Suppl. S4), 124–133. [[CrossRef](#)]
21. Schmitt, C.M.; Doering, H.; Schmidt, T.; Lutz, R.; Neukam, F.W.; Schlegel, K.A. Histological results after maxillary sinus augmentation with Straumann®BoneCeramic, Bio-Oss®, Puros®, and autologous bone. A randomized controlled clinical trial. *Clin. Oral Implant. Res.* **2013**, *24*, 576–585. [[CrossRef](#)] [[PubMed](#)]
22. Maiorana, C.; Ferrario, S.; Poli, P.P.; Manfredini, M. Autogenous Chin Block Grafts in the Aesthetic Zone: A 20-Year Follow-Up Case Report. *Case Rep. Dent.* **2020**, *2020*, 6525797. [[CrossRef](#)]
23. Reininger, D.; Cobo-Vázquez, C.; Rosenberg, B.; López-Quiles, J. Alternative intraoral donor sites to the chin and mandibular body-ramus. *J. Clin. Exp. Dent.* **2017**, *9*, e1474–e1481. [[CrossRef](#)] [[PubMed](#)]
24. Sakkas, A.; Wilde, F.; Heufelder, M.; Winter, K.; Schramm, A. Autogenous bone grafts in oral implantology—Is it still a “gold standard”? A consecutive review of 279 patients with 456 clinical procedures. *Int. J. Implant. Dent.* **2017**, *3*, 23. [[CrossRef](#)]
25. Titsinides, S.; Agrogiannis, G.; Karatzas, T. Bone grafting materials in dentoalveolar reconstruction: A comprehensive review. *Jpn. Dent. Sci. Rev.* **2019**, *55*, 26–32. [[CrossRef](#)]
26. Wortmann, D.E.; Klein-Nulend, J.; van Ruijven, L.J.; Schortinghuis, J.; Vissink, A.; Raghoobar, G.M. Incorporation of anterior iliac crest or calvarial bone grafts in reconstructed atrophied maxillae: A randomized clinical trial with histomorphometric and micro-CT analyses. *Clin. Implant. Dent. Relat. Res.* **2021**, *23*, 492–502. [[CrossRef](#)]
27. Annibali, S.; Cristalli, M.P.; La Monaca, G.; Bignozzi, I.; Scarano, A.; Corrado, R.; Muzio, L.L. Human maxillary sinuses augmented with mineralized, solvent-dehydrated bone allograft: A longitudinal case series. *Implant. Dent.* **2011**, *20*, 445–454. [[CrossRef](#)] [[PubMed](#)]
28. Bavetta, G. The use of human allogenic graft (HBA) for maxillary bone regeneration: Review of literature and case reports. *Curr. Pharm. Des.* **2012**, *18*, 5559–5568. [[CrossRef](#)]
29. Irinakis, T. Efficacy of injectable demineralized bone matrix as graft material during sinus elevation surgery with simultaneous implant placement in the posterior maxilla: Clinical evaluation of 49 sinuses. *J. Oral Maxillofac. Surg.* **2011**, *69*, 134–141. [[CrossRef](#)]
30. Chaushu, L.; Silva, E.R.; Balan, V.F.; Chaushu, G.; Xavier, S.P. Sinus augmentation-autograft vs. fresh frozen allograft: Bone density dynamics and implant stability. *J. Stomatol. Oral Maxillofac. Surg.* **2021**, *122*, 467–471. [[CrossRef](#)]
31. Roberts, T.T.; Rosenbaum, A.J. Bone grafts, bone substitutes and orthobiologics. *Organogenesis* **2012**, *8*, 114–124. [[CrossRef](#)]
32. Özkan, Y.; Akoğlu, B.; Kulak-Özkan, Y. Maxillary sinus floor augmentation using bovine bone grafts with simultaneous implant placement: A 5-year prospective follow-up study. *Implant. Dent.* **2011**, *20*, 455–459. [[CrossRef](#)]
33. Scarano, A.; Piattelli, A.; Perrotti, V.; Manzon, L.; Iezzi, G. Maxillary sinus augmentation in humans using cortical porcine bone: A histological and histomorphometrical evaluation after 4 and 6 months. *Clin. Implant. Dent. Relat. Res.* **2011**, *13*, 13–18. [[CrossRef](#)]
34. Sivolella, S.; Bressan, E.; Gnocco, E.; Berengo, M.; Favero, G.A. Maxillary sinus augmentation with bovine bone and simultaneous dental implant placement in conditions of severe alveolar atrophy: A retrospective analysis of a consecutively treated case series. *Quintessence Int.* **2011**, *42*, 851–862. [[PubMed](#)]
35. Temmerman, A.; Cortellini, S.; Van Dessel, J.; De Greef, A.; Jacobs, R.; Dhondt, R.; Teughels, W.; Quirynen, M. Bovine-derived xenograft in combination with autogenous bone chips versus xenograft alone for the augmentation of bony dehiscences around oral implants: A randomized, controlled, split-mouth clinical trial. *J. Clin. Periodontol.* **2020**, *47*, 110–119. [[CrossRef](#)] [[PubMed](#)]
36. Testori, T.; Iezzi, G.; Manzon, L.; Fratto, G.; Piattelli, A.; Weinstein, R.L. High temperature-treated bovine porous hydroxyapatite in sinus augmentation procedures: A case report. *Int. J. Periodontics Restor. Dent.* **2012**, *32*, 295–301.
37. Kuchler, U.; Dos Santos, G.M.; Heimel, P.; Stähli, A.; Strauss, F.J.; Tangl, S.; Gruber, R. DBBM shows no signs of resorption under inflammatory conditions. An experimental study in the mouse calvaria. *Clin. Oral Implant. Res.* **2020**, *31*, 10–17. [[CrossRef](#)]
38. Kuchler, U.; Heimel, P.; Stähli, A.; Strauss, F.J.; Luza, B.; Gruber, R. Impact of DBBM Fragments on the Porosity of the Calvarial Bone: A Pilot Study on Mice. *Materials* **2020**, *13*, 4748. [[CrossRef](#)]

39. Sheikh, Z.; Hamdan, N.; Abdallah, M.-N.; Glogauer, M.; Grynypas, M. Natural and synthetic bone replacement graft materials for dental and maxillofacial applications. In *Advanced Dental Biomaterials*; Khurshid, Z., Najeeb, S., Zafar, M.S., Sefat, F., Eds.; Woodhead Publishing: Sawston, UK, 2019; pp. 347–376.
40. Kolk, A.; Handschel, J.; Drescher, W.; Rothamel, D.; Kloss, F.; Blessmann, M.; Heiland, M.; Wolff, K.-D.; Smeets, R. Current trends and future perspectives of bone substitute materials—from space holders to innovative biomaterials. *J. Cranio-Maxillofac. Surg.* **2012**, *40*, 706–718. [[CrossRef](#)]
41. Wang, W.; Yeung, K.W.K. Bone grafts and biomaterials substitutes for bone defect repair: A review. *Bioact. Mater.* **2017**, *2*, 224–247. [[CrossRef](#)]
42. Temmerman, A.; Hertelé, S.; Teughels, W.; Dekeyser, C.; Jacobs, R.; Quirynen, M. Are panoramic images reliable in planning sinus augmentation procedures? *Clin. Oral Implant. Res.* **2011**, *22*, 189–194. [[CrossRef](#)] [[PubMed](#)]
43. Bornstein, M.M.; Horner, K.; Jacobs, R. Use of cone beam computed tomography in implant dentistry: Current concepts, indications and limitations for clinical practice and research. *Periodontology 2000* **2017**, *73*, 51–72. [[CrossRef](#)]
44. Bornstein, M.M.; Scarfe, W.C.; Vaughn, V.M.; Jacobs, R. Cone beam computed tomography in implant dentistry: A systematic review focusing on guidelines, indications, and radiation dose risks. *Int. J. Oral Maxillofac. Implant.* **2014**, *29*, 55–77. [[CrossRef](#)]
45. Jacobs, R.; Salmon, B.; Codari, M.; Hassan, B.; Bornstein, M.M. Cone beam computed tomography in implant dentistry: Recommendations for clinical use. *BMC Oral Health* **2018**, *18*, 88. [[CrossRef](#)]
46. Reddy, M.S.; Mayfield-Donahoo, T.; Vandervan, F.J.; Jeffcoat, M.K. A comparison of the diagnostic advantages of panoramic radiography and computed tomography scanning for placement of root form dental implants. *Clin. Oral Implant. Res.* **1994**, *5*, 229–238. [[CrossRef](#)] [[PubMed](#)]
47. Arias-Irimia, Ó.; Barona Dorado, C.; Gómez Moreno, G.; Brinkmann, J.C.; Martínez-González, J.M. Pre-operative measurement of the volume of bone graft in sinus lifts using CompuDent. *Clin. Oral Implant. Res.* **2012**, *23*, 1070–1074. [[CrossRef](#)] [[PubMed](#)]
48. Buyukkurt, M.C.; Tozoglu, S.; Yavuz, M.S.; Aras, M.H. Simulation of sinus floor augmentation with symphysis bone graft using three-dimensional computerized tomography. *Int. J. Oral Maxillofac. Surg.* **2010**, *39*, 788–792. [[CrossRef](#)]
49. Krennmair, G.; Krainhöfner, M.; Maier, H.; Weinländer, M.; Piehslinger, E. Computerized tomography-assisted calculation of sinus augmentation volume. *Int. J. Oral Maxillofac. Implant.* **2006**, *21*, 907–913.
50. Uchida, Y.; Goto, M.; Katsuki, T.; Soejima, Y. Measurement of maxillary sinus volume using computerized tomographic images. *Int. J. Oral Maxillofac. Implant.* **1998**, *13*, 811–818.
51. Scarfe, W.C.; Farman, A.G. What is cone-beam CT and how does it work? *Dent. Clin. N. Am.* **2008**, *52*, 707–730. [[CrossRef](#)]
52. Scarfe, W.C.; Farman, A.G.; Sukovic, P. Clinical applications of cone-beam computed tomography in dental practice. *J. Can. Dent. Assoc.* **2006**, *72*, 75–80. [[PubMed](#)]
53. White, S.C.; Pharoah, M.J. *White and Pharoah's Oral Radiology: Principles and Interpretation*; Elsevier Health Sciences: Amsterdam, The Netherlands, 2018; pp. 418–444.
54. Pauwels, R.; Jacobs, R.; Singer, S.R.; Mupparapu, M. CBCT-based bone quality assessment: Are Hounsfield units applicable? *Dentomaxillofacial Radiol.* **2015**, *44*, 20140238. [[CrossRef](#)]
55. Tyndall, D.A.; Price, J.B.; Tetradis, S.; Ganz, S.D.; Hildebolt, C.; Scarfe, W.C. Position statement of the American Academy of Oral and Maxillofacial Radiology on selection criteria for the use of radiology in dental implantology with emphasis on cone beam computed tomography. *Oral Surg. Oral Med. Oral Pathol. Oral Radiol.* **2012**, *113*, 817–826. [[CrossRef](#)]
56. Harris, D.; Horner, K.; Gröndahl, K.; Jacobs, R.; Helmrot, E.; Benic, G.I.; Bornstein, M.M.; Dawood, A.; Quirynen, M.E.A.O. guidelines for the use of diagnostic imaging in implant dentistry 2011. A consensus workshop organized by the European Association for Osseointegration at the Medical University of Warsaw. *Clin. Oral Implant. Res.* **2012**, *23*, 1243–1253. [[CrossRef](#)] [[PubMed](#)]
57. Oenning, A.C.; Jacobs, R.; Pauwels, R.; Stratis, A.; Hedesi, M.; Salmon, B. Cone-beam CT in paediatric dentistry: DIMITRA project position statement. *Pediatr. Radiol.* **2018**, *48*, 308–316. [[CrossRef](#)]
58. Oenning, A.C.; Jacobs, R.; Salmon, B. ALADAIP, beyond ALARA and towards personalized optimization for paediatric cone-beam CT. *Int. J. Paediatr. Dent.* **2021**, *31*, 676–678. [[CrossRef](#)]
59. Carmeli, G.; Artzi, Z.; Kozlovsky, A.; Segev, Y.; Landsberg, R. Antral computerized tomography pre-operative evaluation: Relationship between mucosal thickening and maxillary sinus function. *Clin. Oral Implant. Res.* **2011**, *22*, 78–82. [[CrossRef](#)] [[PubMed](#)]
60. Janner, S.F.; Caversaccio, M.D.; Dubach, P.; Sendi, P.; Buser, D.; Bornstein, M.M. Characteristics and dimensions of the Schneiderian membrane: A radiographic analysis using cone beam computed tomography in patients referred for dental implant surgery in the posterior maxilla. *Clin. Oral Implant. Res.* **2011**, *22*, 1446–1453. [[CrossRef](#)]
61. Pignataro, L.; Mantovani, M.; Torretta, S.; Felisati, G.; Sambataro, G. ENT assessment in the integrated management of candidate for (maxillary) sinus lift. *Acta Otorhinolaryngol. Ital.* **2008**, *28*, 110–119.
62. Ribeiro-Rotta, R.F.; Lindh, C.; Pereira, A.C.; Rohlin, M. Ambiguity in bone tissue characteristics as presented in studies on dental implant planning and placement: A systematic review. *Clin. Oral Implant. Res.* **2011**, *22*, 789–801. [[CrossRef](#)]
63. Pauwels, R.; Araki, K.; Siewerdsen, J.H.; Thongvigitmanee, S.S. Technical aspects of dental CBCT: State of the art. *Dentomaxillofacial Radiol.* **2015**, *44*, 20140224. [[CrossRef](#)]

64. Loubele, M.; Bogaerts, R.; Van Dijck, E.; Pauwels, R.; Vanheusden, S.; Suetens, P.; Marchal, G.; Sanderink, G.; Jacobs, R. Comparison between effective radiation dose of CBCT and MSCT scanners for dentomaxillofacial applications. *Eur. J. Radiol.* **2009**, *71*, 461–468. [[CrossRef](#)]
65. Rahpeyma, A.; Khajehahmadi, S. Open Sinus Lift Surgery and the Importance of Preoperative Cone-Beam Computed Tomography Scan: A Review. *J. Int. Oral Health* **2015**, *7*, 127–133.
66. Ducommun, J.; Bornstein, M.M.; Wong, M.C.M.; von Arx, T. Distances of root apices to adjacent anatomical structures in the anterior maxilla: An analysis using cone beam computed tomography. *Clin. Oral Investig.* **2019**, *23*, 2253–2263. [[CrossRef](#)] [[PubMed](#)]
67. Kahnberg, K.-E.; Wallström, M.; Rasmusson, L. Local sinus lift for single-tooth implant. I. clinical and radiographic follow-up. *Clin. Implant. Dent. Relat. Res.* **2011**, *13*, 231–237. [[CrossRef](#)]
68. Testori, T.; Weinstein, T.; Taschieri, S.; Wallace, S.S. Risk factors in lateral window sinus elevation surgery. *Periodontology* **2000** *2019*, *81*, 91–123. [[CrossRef](#)]
69. Janner, S.F.M.; Dubach, P.; Suter, V.G.A.; Caversaccio, M.D.; Buser, D.; Bornstein, M.M. Sinus floor elevation or referral for further diagnosis and therapy: A comparison of maxillary sinus assessment by ENT specialists and dentists using cone beam computed tomography. *Clin. Oral Implant. Res.* **2020**, *31*, 463–475. [[CrossRef](#)]
70. Becker, S.T.; Terheyden, H.; Steinriede, A.; Behrens, E.; Springer, I.; Wiltfang, J. Prospective observation of 41 perforations of the Schneiderian membrane during sinus floor elevation. *Clin. Oral Implant. Res.* **2008**, *19*, 1285–1289. [[CrossRef](#)]
71. Monje, A.; Diaz, K.T.; Aranda, L.; Insua, A.; Garcia-Nogales, A.; Wang, H.-L. Schneiderian Membrane Thickness and Clinical Implications for Sinus Augmentation: A Systematic Review and Meta-Regression Analyses. *J. Periodontol.* **2016**, *87*, 888–899. [[CrossRef](#)] [[PubMed](#)]
72. Tavelli, L.; Borgonovo, A.E.; Re, D.; Maiorana, C. Sinus presurgical evaluation: A literature review and a new classification proposal. *Minerva Stomatol.* **2017**, *66*, 115–131. [[CrossRef](#)] [[PubMed](#)]
73. Shanbhag, S.; Karnik, P.; Shirke, P.; Shanbhag, V. Cone-beam computed tomographic analysis of sinus membrane thickness, ostium patency, and residual ridge heights in the posterior maxilla: Implications for sinus floor elevation. *Clin. Oral Implant. Res.* **2013**, *25*, 755–760. [[CrossRef](#)] [[PubMed](#)]
74. Bornstein, M.M.; Seiffert, C.; Maestre-Ferrin, L.; Fodich, I.; Jacobs, R.; Buser, D.; Von Arx, T. An Analysis of Frequency, Morphology, and Locations of Maxillary Sinus Septa Using Cone Beam Computed Tomography. *Int. J. Oral Maxillofac. Implant.* **2016**, *31*, 280–287. [[CrossRef](#)]
75. Schriber, M.; Von Arx, T.; Sendi, P.; Jacobs, R.; Suter, V.G.; Bornstein, M.M. Evaluating Maxillary Sinus Septa Using Cone Beam Computed Tomography: Is There a Difference in Frequency and Type Between the Dentate and Edentulous Posterior Maxilla? *Int. J. Oral Maxillofac. Implant.* **2017**, *32*, 1324–1332. [[CrossRef](#)]
76. Neugebauer, J.; Ritter, L.; Mischkowski, R.A.; Dreiseidler, T.; Scherer, P.; Ketterle, M.; Rothamel, D.; Zöller, J.E. Evaluation of maxillary sinus anatomy by cone-beam CT prior to sinus floor elevation. *Int. J. Oral Maxillofac. Implant.* **2010**, *25*, 258–265.
77. Zijderveld, S.A.; van den Bergh, J.P.; Schulten, E.A.; ten Bruggenkate, C.M. Anatomical and surgical findings and complications in 100 consecutive maxillary sinus floor elevation procedures. *J. Oral Maxillofac. Surg.* **2008**, *66*, 1426–1438. [[CrossRef](#)]
78. Yeung, A.W.K.; Colsool, N.; Montalva, C.; Hung, K.; Jacobs, R.; Bornstein, M.M. Visibility, location, and morphology of the primary maxillary sinus ostium and presence of accessory ostia: A retrospective analysis using cone beam computed tomography (CBCT). *Clin. Oral Investig.* **2019**, *23*, 3977–3986. [[CrossRef](#)]
79. Chan, H.-L.; Suarez, F.; Monje, A.; Benavides, E.; Wang, H.-L. Evaluation of maxillary sinus width on cone-beam computed tomography for sinus augmentation and new sinus classification based on sinus width. *Clin. Oral Implant. Res.* **2012**, *25*, 647–652. [[CrossRef](#)] [[PubMed](#)]
80. Lim, E.L.; Ngeow, W.C.; Lim, D. The implications of different lateral wall thicknesses on surgical access to the maxillary sinus. *Braz. Oral Res.* **2017**, *31*, e97. [[CrossRef](#)] [[PubMed](#)]
81. Varela-Centelles, P.; Loira, M.; González-Mosquera, A.; Romero-Mendez, A.; Seoane, J.; García-Pola, M.J.; Seoane-Romero, J.M. Study of factors influencing preoperative detection of alveolar antral artery by CBCT in sinus floor elevation. *Sci. Rep.* **2020**, *10*, 10820. [[CrossRef](#)] [[PubMed](#)]
82. Greenstein, G.; Cavallaro, J.; Tarnow, D. Practical application of anatomy for the dental implant surgeon. *J. Periodontol.* **2008**, *79*, 1833–1846. [[CrossRef](#)]
83. Jacobs, R.; Scarfe, W.C. Dental Implants. In *Maxillofacial Cone Beam Computed Tomography: Principles, Techniques and Clinical Applications*; Scarfe, W.C., Angelopoulos, C., Eds.; Springer International Publishing: Cham, Switzerland, 2018; pp. 745–830.
84. Abdel-Wahed, N.A.; Bahammam, M.A. Cone Beam CT-Based Preoperative Volumetric Estimation of Bone Graft Required for Lateral Window Sinus Augmentation, Compared with Intraoperative Findings: A Pilot Study. *Open Dent. J.* **2018**, *12*, 820–826. [[CrossRef](#)]
85. Binshabaib, M.; Alharthi, S.; Alkraid, R.; Aljared, S.; Alshami, A.; Mansour, S. Incidental findings in maxillary sinus area on cone-beam-computed-tomographic-scans: A retrospective study with emphasis on gender and ethnicity. *Saudi Dent. J.* **2021**, *33*, 184–187. [[CrossRef](#)]
86. Pazera, P.; Bornstein, M.M.; Pazera, A.; Sendi, P.; Katsaros, C. Incidental maxillary sinus findings in orthodontic patients: A radiographic analysis using cone-beam computed tomography (CBCT). *Orthod. Craniofacial Res.* **2011**, *14*, 17–24. [[CrossRef](#)] [[PubMed](#)]

87. Vandenberghe, B. The digital patient—Imaging science in dentistry. *J. Dent.* **2018**, *74* (Suppl. S1), S21–S26. [[CrossRef](#)]
88. Lin, Y.-M. Digitalisation in Dentistry: Development and Practices. In *The Digitization of Business in China: Exploring the Transformation from Manufacturing to a Digital Service Hub*; Kim, Y.-C., Chen, P.-C., Eds.; Springer International Publishing: Cham, Switzerland, 2018; pp. 199–217.
89. Shujaat, S.; Bornstein, M.M.; Price, J.B.; Jacobs, R. Integration of imaging modalities in digital dental workflows—possibilities, limitations, and potential future developments. *Dentomaxillofacial Radiol.* **2021**, *50*, 20210268. [[CrossRef](#)] [[PubMed](#)]
90. Shujaat, S.; Riaz, M.; Jacobs, R. Synergy between artificial intelligence and precision medicine for computer-assisted oral and maxillofacial surgical planning. *Clin. Oral Investig.* **2023**, *27*, 897–906. [[CrossRef](#)] [[PubMed](#)]
91. Heye, T.; Merkle, E.M.; Reiner, C.S.; Davenport, M.S.; Horvath, J.J.; Feuerlein, S.; Breault, S.R.; Gall, P.; Bashir, M.R.; Dale, B.M.; et al. Reproducibility of dynamic contrast-enhanced MR imaging. Part II. Comparison of intra- and interobserver variability with manual region of interest placement versus semiautomatic lesion segmentation and histogram analysis. *Radiology* **2013**, *266*, 812–821. [[CrossRef](#)] [[PubMed](#)]
92. Parmar, C.; Velazquez, E.R.; Leijenaar, R.; Jermoumi, M.; Carvalho, S.; Mak, R.H.; Mitra, S.; Shankar, B.U.; Kikinis, R.; Haibe-Kains, B.; et al. Robust Radiomics feature quantification using semiautomatic volumetric segmentation. *PLoS ONE* **2014**, *9*, e102107. [[CrossRef](#)]
93. Renard, F.; Guedria, S.; De Palma, N.; Vuillerme, N. Variability and reproducibility in deep learning for medical image segmentation. *Sci. Rep.* **2020**, *10*, 13724. [[CrossRef](#)]
94. Withey, D.; Koles, Z. Medical Image Segmentation: Methods and Software. In Proceedings of the 2007 Joint Meeting of the 6th International Symposium on Noninvasive Functional Source Imaging of the Brain and Heart and the International Conference on Functional Biomedical Imaging, Hangzhou, China, 12–14 October 2007; pp. 140–143. [[CrossRef](#)]
95. Choi, H.; Jeon, K.J.; Kim, Y.H.; Ha, E.-G.; Lee, C.; Han, S.-S. Deep learning-based fully automatic segmentation of the maxillary sinus on cone-beam computed tomographic images. *Sci. Rep.* **2022**, *12*, 14009. [[CrossRef](#)] [[PubMed](#)]
96. Hung, K.F.; Ai, Q.Y.H.; King, A.D.; Bornstein, M.M.; Wong, L.M.; Leung, Y.Y. Automatic detection and segmentation of morphological changes of the maxillary sinus mucosa on cone-beam computed tomography images using a three-dimensional convolutional neural network. *Clin. Oral Investig.* **2022**, *26*, 3987–3998. [[CrossRef](#)] [[PubMed](#)]
97. Jung, S.-K.; Lim, H.-K.; Lee, S.; Cho, Y.; Song, I.-S. Deep Active Learning for Automatic Segmentation of Maxillary Sinus Lesions Using a Convolutional Neural Network. *Diagnostics* **2021**, *11*, 688. [[CrossRef](#)]
98. Cecchetti, F.; Spuntarelli, M.; Mazza, D.; Di Girolamo, M.; Baggi, L. Guided sinus lift: Virtual planning of surgical templates for lateral access. *J. Biol. Regul. Homeost. Agents* **2021**, *35*, 139–145. [[CrossRef](#)] [[PubMed](#)]
99. Mandelaris, G.A.; Rosenfeld, A.L. A novel approach to the antral sinus bone graft technique: The use of a prototype cutting guide for precise outlining of the lateral wall. A case report. *Int. J. Periodontics Restor. Dent.* **2008**, *28*, 569–575.
100. Pistilli, R.; Canullo, L.; Pesce, P.; Pistilli, V.; Caponio, V.C.A.; Sbricoli, L. Guided implant surgery and sinus lift in severely resorbed maxillae: A retrospective clinical study with up to 10 years of follow-up. *J. Dent.* **2022**, *121*, 104137. [[CrossRef](#)]
101. Strbac, G.D.; Giannis, K.; Schnappauf, A.; Bertl, K.; Stavropoulos, A.; Ulm, C. Guided Lateral Sinus Lift Procedure Using 3-Dimensionally Printed Templates for a Safe Surgical Approach: A Proof-of-Concept Case Report. *J. Oral Maxillofac. Surg.* **2020**, *78*, 1529–1537. [[CrossRef](#)]
102. Osman, A.H.; Mansour, H.; Atef, M.; Hakam, M. Computer guided sinus floor elevation through lateral window approach with simultaneous implant placement. *Clin. Implant. Dent. Relat. Res.* **2017**, *20*, 137–143. [[CrossRef](#)]
103. Pozzi, A.; Moy, P.K. Minimally Invasive Transcrestal Guided Sinus Lift (TGSL): A Clinical Prospective Proof-of-Concept Cohort Study up to 52 Months. *Clin. Implant. Dent. Relat. Res.* **2013**, *16*, 582–593. [[CrossRef](#)]
104. An, X.; Lee, C.; Fang, Y.; Choi, B. Immediate nonfunctional loading of implants placed simultaneously using computer-guided flapless maxillary crestal sinus augmentation with bone morphogenetic protein-2/collagen matrix. *Clin. Implant. Dent. Relat. Res.* **2019**, *21*, 1054–1061. [[CrossRef](#)]
105. Mauer, R.G.; Shadrav, A.; Dashti, M. Static Surgical Guides and Dynamic Navigation in Implant Surgery. In *Navigation in Oral and Maxillofacial Surgery: Applications, Advances, and Limitations*; Parhiz, S.A., James, J.N., Ghasemi, S., Amirzade-Irani, M.H., Eds.; Springer International Publishing: Cham, Switzerland, 2022; pp. 135–150.
106. Block, M.S.; Emery, R.W.; Cullum, D.R.; Sheikh, A. Implant Placement Is More Accurate Using Dynamic Navigation. *J. Oral Maxillofac. Surg.* **2017**, *75*, 1377–1386. [[CrossRef](#)]
107. Wu, B.-Z.; Ma, F.-F.; Sun, F. Analysis of the accuracy of a dynamic navigation system when performing dental implant surgery with transcrestal sinus floor elevation: A pilot study. *J. Dent. Sci.* **2023**. [[CrossRef](#)]
108. Blake, F.; Blessmann, M.; Pohlenz, P.; Heiland, M. A new imaging modality for intraoperative evaluation of sinus floor augmentation. *Int. J. Oral Maxillofac. Surg.* **2008**, *37*, 183–185. [[CrossRef](#)] [[PubMed](#)]
109. Dellavia, C.; Speroni, S.; Pellegrini, G.; Gatto, A.; Maiorana, C. A New Method to Evaluate Volumetric Changes in Sinus Augmentation Procedure. *Clin. Implant. Dent. Relat. Res.* **2013**, *16*, 684–690. [[CrossRef](#)] [[PubMed](#)]
110. Diserens, V.; Mericske, E.; Mericske-Stern, R. Radiographic Analysis of the Transcrestal Sinus Floor Elevation: Short-Term Observations. *Clin. Implant. Dent. Relat. Res.* **2005**, *7*, 70–78. [[CrossRef](#)]
111. Gray, C.F.; Redpath, T.W.; Bainton, R.; Smith, F.W. Magnetic resonance imaging assessment of a sinus lift operation using reoxidised cellulose (SurgicelR) as graft material. *Clin. Oral Implant. Res.* **2001**, *12*, 526–530. [[CrossRef](#)]

112. Hallman, M.; Hedin, M.; Sennerby, L.; Lundgren, S. A prospective 1-year clinical and radiographic study of implants placed after maxillary sinus floor augmentation with bovine hydroxyapatite and autogenous bone. *J. Oral Maxillofac. Surg.* **2002**, *60*, 277–284. [[CrossRef](#)]
113. Johansson, B.; Grepe, A.; Wannfors, K.; Aberg, P.; Hirsch, J.M. Volumetry of simulated bone grafts in the edentulous maxilla by computed tomography: An experimental study. *Dentomaxillofacial Radiol.* **2001**, *30*, 153–156. [[CrossRef](#)]
114. Kirmeier, R.; Arnetzl, C.; Robl, T.; Payer, M.; Lorenzoni, M.; Jakse, N. Reproducibility of volumetric measurements on maxillary sinuses. *Int. J. Oral Maxillofac. Surg.* **2011**, *40*, 195–199. [[CrossRef](#)]
115. Klijn, R.J.; Meijer, G.J.; Bronkhorst, E.M.; Jansen, J.A. Sinus Floor Augmentation Surgery Using Autologous Bone Grafts from Various Donor Sites: A Meta-Analysis of the Total Bone Volume. *Tissue Eng. Part B Rev.* **2010**, *16*, 295–303. [[CrossRef](#)]
116. Ozyuvaci, H.; Bilgiç, B.; Firatli, E. Radiologic and Histomorphometric Evaluation of Maxillary Sinus Grafting with Alloplastic Graft Materials. *J. Periodontol.* **2003**, *74*, 909–915. [[CrossRef](#)]
117. Reinert, S.; König, S.; Bremerich, A.; Eufinger, H.; Krimmel, M. Stability of bone grafting and placement of implants in the severely atrophic maxilla. *Br. J. Oral Maxillofac. Surg.* **2003**, *41*, 249–255. [[CrossRef](#)]
118. Riachi, F.; Naaman, N.; Tabarani, C.; Aboelsaad, N.; Aboushelib, M.N.; Berberi, A.; Salameh, Z. Influence of Material Properties on Rate of Resorption of Two Bone Graft Materials after Sinus Lift Using Radiographic Assessment. *Int. J. Dent.* **2012**, *2012*, 737262. [[CrossRef](#)] [[PubMed](#)]
119. Szabó, G.; Huys, L.; Coulthard, P.; Maiorana, C.; Garagiola, U.; Barabás, J.; Németh, Z.; Hrabák, K.; Suba, Z. A prospective multicenter randomized clinical trial of autogenous bone versus beta-tricalcium phosphate graft alone for bilateral sinus elevation: Histologic and histomorphometric evaluation. *Int. J. Oral Maxillofac. Implant.* **2005**, *20*, 371–381.
120. Wanschitz, F.; Figl, M.; Wagner, A.; Rolf, E. Measurement of volume changes after sinus floor augmentation with a phycogenic hydroxyapatite. *Int. J. Oral Maxillofac. Implant.* **2006**, *21*, 433–438.
121. Zijderveld, S.A.; Schulten, E.A.J.M.; Aartman, I.H.A.; ten Bruggenkate, C.M. Long-term changes in graft height after maxillary sinus floor elevation with different grafting materials: Radiographic evaluation with a minimum follow-up of 4.5 years. *Clin. Oral Implant. Res.* **2009**, *20*, 691–700. [[CrossRef](#)]
122. Hatano, N.; Shimizu, Y.; Ooya, K. A clinical long-term radiographic evaluation of graft height changes after maxillary sinus floor augmentation with a 2: 1 autogenous bone/xenograft mixture and simultaneous placement of dental implants. *Clin. Oral Implant. Res.* **2004**, *15*, 339–345. [[CrossRef](#)]
123. Hürzeler, M.B.; Kirsch, A.; Ackermann, K.L.; Quiñones, C.R. Reconstruction of the severely resorbed maxilla with dental implants in the augmented maxillary sinus: A 5-year clinical investigation. *Int. J. Oral Maxillofac. Implant.* **1996**, *11*, 466–475.
124. Galindo-Moreno, P.; Hernández-Cortés, P.; Mesa, F.; Carranza, N.; Juodžbalys, G.; Aguilar, M.; Dds, P.G.; Hernández-Cortés, P. Slow Resorption of Anorganic Bovine Bone by Osteoclasts in Maxillary Sinus Augmentation. *Clin. Implant. Dent. Relat. Res.* **2012**, *15*, 858–866. [[CrossRef](#)]
125. Kirmeier, R.; Payer, M.; Wehrsuetz, M.; Jakse, N.; Platzer, S.; Lorenzoni, M. Evaluation of three-dimensional changes after sinus floor augmentation with different grafting materials. *Clin. Oral Implant. Res.* **2008**, *19*, 366–372. [[CrossRef](#)]
126. Mazzocco, F.; Lops, D.; Gobbato, L.; Lolato, A.; Romeo, E.; Del Fabbro, M. Three-Dimensional Volume Change of Grafted Bone in the Maxillary Sinus. *Int. J. Oral Maxillofac. Implant.* **2014**, *29*, 178–184. [[CrossRef](#)]
127. Molina, A.; Sanz-Sánchez, I.; Sanz-Martín, I.; Ortiz-Vigón, A.; Sanz, M. Complications in sinus lifting procedures: Classification and management. *Periodontology 2000* **2022**, *88*, 103–115. [[CrossRef](#)]
128. Zhou, C.; Sun, S.-Z.; Lin, M.-N.; He, F.-M. Responses of Sinus Membrane and Antral Pseudocyst Following Lateral Window Sinus Augmentation with Bone Grafting: A Retrospective Study. *Int. J. Oral Maxillofac. Implant.* **2021**, *36*, 885–893. [[CrossRef](#)]
129. Jiang, X.; He, S.; Bornstein, M.M.; Wu, Y.; Ye, L.; Wang, F. Effects of different grafting materials on volumetric changes in the Schneiderian membrane following lateral maxillary sinus floor elevation: A preliminary study. *BMC Oral Health* **2023**, *23*, 102. [[CrossRef](#)]
130. Gillies, R.J.; Kinahan, P.E.; Hricak, H. Radiomics: Images Are More than Pictures, They Are Data. *Radiology* **2016**, *278*, 563–577. [[CrossRef](#)]
131. Leite, A.F.; Vasconcelos, K.D.F.; Willems, H.; Jacobs, R. Radiomics and Machine Learning in Oral Healthcare. *Proteom. Clin. Appl.* **2020**, *14*, e1900040. [[CrossRef](#)]
132. Santos, G.N.M.; da Silva, H.E.C.; Ossege, F.E.L.; Figueiredo, P.T.D.S.; Melo, N.D.S.; Stefani, C.M.; Leite, A.F. Radiomics in bone pathology of the jaws. *Dentomaxillofacial Radiol.* **2023**, *52*, 20220225. [[CrossRef](#)]

**Disclaimer/Publisher’s Note:** The statements, opinions and data contained in all publications are solely those of the individual author(s) and contributor(s) and not of MDPI and/or the editor(s). MDPI and/or the editor(s) disclaim responsibility for any injury to people or property resulting from any ideas, methods, instructions or products referred to in the content.